

## NANO-AMPÈRE STIMULATION WINDOW FOR CULTURED NEURONS ON MICRO-ELECTRODE ARRAYS

J.R. Buitenweg<sup>1</sup>, W.L.C. Rutten<sup>1</sup>, E. Marani<sup>1,2</sup>

<sup>1</sup>Institute for Biomedical Technology, Faculty of Electrical Engineering, University of Twente, Enschede, The Netherlands

<sup>2</sup>Neuroregulation Group, dept. of Neurosurgery, Leiden University Medical Centre, The Netherlands

**Abstract-** From experiments, it appears to be possible to stimulate a neuron by depolarisation of the lower membrane patch, the sealing part of the membrane, using a nano-ampère current through the extracellular electrode. Also, a stimulation window is observed. These findings can be explained by a finite element model of the neuron-electrode interface which permits geometry based dynamic modeling of the neuron-electrode interface and can be used to explore the requirements for lower membrane stimulation in more detail. An intracellular action potential develops if the current through the lower membrane is able to depolarize the upper membrane sufficiently.

**Keywords** – multi-electrode arrays, cultured neurons, neuron-electrode contact, sealing, extracellular stimulation

### I. INTRODUCTION

Planar micro-electrode arrays (MEAs) have become a common tool for establishing single cell electrical contacts with cultured neurons. Especially the feasibility of long term recording of bioelectrical activity has been demonstrated by several groups [1,2]. However, the conditions for reliable and selective stimulation of cultured neurons are poorly understood.

This paper reports on extracellular stimulation of cultured neurons sealing a microelectrode. The experimental results will be explained using a finite element model of the neuron-electrode interface. This model permits dynamic simulation of the local membrane potentials and current densities due to extracellular stimulation. The interface geometry, the conductivity of the sealing gap, the local membrane properties and the intracellular or the extracellular stimulation currents are all included in the model.

### II. METHODOLOGY

#### A. Experiments

Dorsal root ganglions were dissected from neonatal (P3) rats, dissociated and purified by removing non-neuronal cells and plated on a MEA with 61 hexagonally ordered electrodes of 5  $\mu\text{m}$  in radius. Electrodes which are completely covered by a neuron were selected for extracellular stimulation (fig. 1). The intracellular potential of the neuron was measured using a micropipette making a whole cell current clamp configuration. Extracellular current stimulation was applied by applying voltage pulses with a duration of 1 ms via a series resistance of 50 MO.

This work was supported by the BIOMED II EC project, shared cost contract no. BMH4-2723.

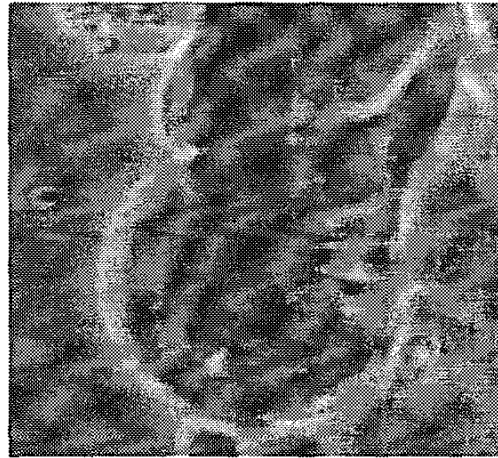


Fig. 1. Neuron from a dorsal root ganglion of a neonatal (P3) rat cultured on top of a planar micro-electrode of 5  $\mu\text{m}$  radius. A micropipette is attached and a whole cell current clamp configuration is established.

#### B. Modeling

The neuron is modeled as a circular soma of radius  $r_c=15 \mu\text{m}$ , with a parabolic profile,  $h_c=10 \mu\text{m}$  (fig. 2). The axon and dendrites of the neuron are not included in this version of the model, since we are primarily interested in situations in which neurons cover electrodes completely or partially. The neuron is positioned with an eccentricity,  $x_c=0$ , on top of an electrode with radius  $r_e=5 \mu\text{m}$ . A sealing gap of thickness  $d_g=100 \text{ nm}$  is modeled between the soma and the substrate.

The medium surrounding the interface is represented by a 3D volume conductor (fig. 3). This volume is meshed and filled with tetrahedral shaped volume elements which permit numerical solutions of the Poisson equation:

$$\nabla \cdot (\sigma \nabla V) = 0 \quad (1)$$

with  $V$  the electrical potential and  $\sigma$  the conductivity of the

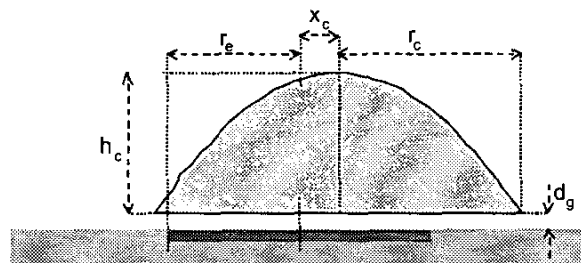


Fig. 2. Parametrical geometry of the neuron-electrode interface.

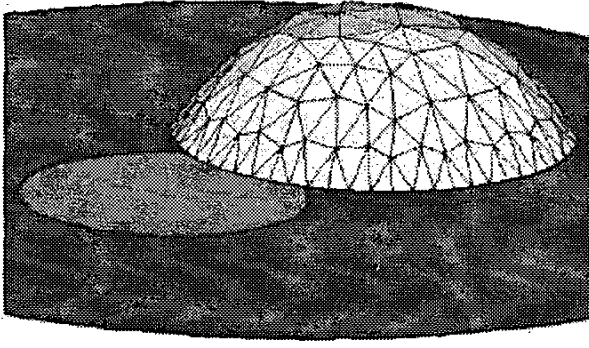


Fig. 3. 3D visualization of the neuron electrode interface geometry as implemented in the finite element model.

medium. The nodes at the outer boundary of the volume conductor are set to zero potential, representing a distant counter electrode. A relationship is formulated between the potentials  $\bar{u}_m$  at the membrane nodes,  $\bar{u}_s$  at the surface of the electrode and the currents into these nodes,  $\bar{i}_m$  and  $\bar{i}_s$  respectively.

$$K_s \cdot \begin{bmatrix} \bar{u}_m \\ \bar{u}_s \\ u_i \\ u_e \end{bmatrix} = \begin{bmatrix} \bar{i}_m \\ \bar{i}_s \\ i_i \\ i_e \end{bmatrix} \quad (2)$$

In this relationship, all membrane potentials are defined with respect to the intracellular potential  $u_i$ , which is represented by a single node, separate from the extracellular volume

conductor. All potentials at the electrode surface are defined with respect to the electrode metal potential  $u_e$ . Extracellular stimulation is applied by injecting a current  $i_e$  into this node.

When  $\bar{u}_m$ ,  $\bar{u}_s$ ,  $i_i$  and  $i_e$  are known, the local membrane and electrode currents follow from

$$\begin{bmatrix} \bar{i}_m \\ \bar{i}_s \end{bmatrix} = K_{mm} \cdot \begin{bmatrix} \bar{u}_m \\ \bar{u}_s \end{bmatrix} + K_{mi} \cdot \begin{bmatrix} i_i \\ i_e \end{bmatrix} \quad (3)$$

with  $K_{mm}$  and  $K_{mi}$  derived from  $K_s$ . Furthermore, the electrode potential and intracellular potential are computed as

$$\begin{bmatrix} u_i \\ u_e \end{bmatrix} = K_{mei} \cdot \begin{bmatrix} \bar{u}_m \\ \bar{u}_s \end{bmatrix} + K_{iei} \cdot \begin{bmatrix} i_i \\ i_e \end{bmatrix} \quad (4)$$

with  $K_{mei}$  and  $K_{iei}$  derived from  $K_s$ .

The time derivatives of all nodal membrane potentials and channel activation constants are computed from the nodal membrane potentials and currents as described in [3] by

$$\begin{aligned} \frac{du_m}{dt} &= \frac{1}{C_m} [\bar{i}_m - \hat{g}_{Na} m^3 h (u_m - u_{Na}) - \hat{g}_K n^4 (u_m - u_K) - \hat{g}_{Cl} (u_m - u_{Cl})] \\ \frac{dh}{dt} &= \frac{\lambda_h (h_\infty(u_m) - h)}{\tau_h(u_m)} \\ \frac{dn}{dt} &= \frac{\lambda_n (n_\infty(u_m) - n)}{\tau_n(u_m)} \end{aligned} \quad (5)$$

with  $h$  and  $n$  the  $\text{Na}^+$  inactivation and  $\text{K}^+$  activation constants. The  $\text{Na}^+$  activation constant  $m$  is considered to be very fast

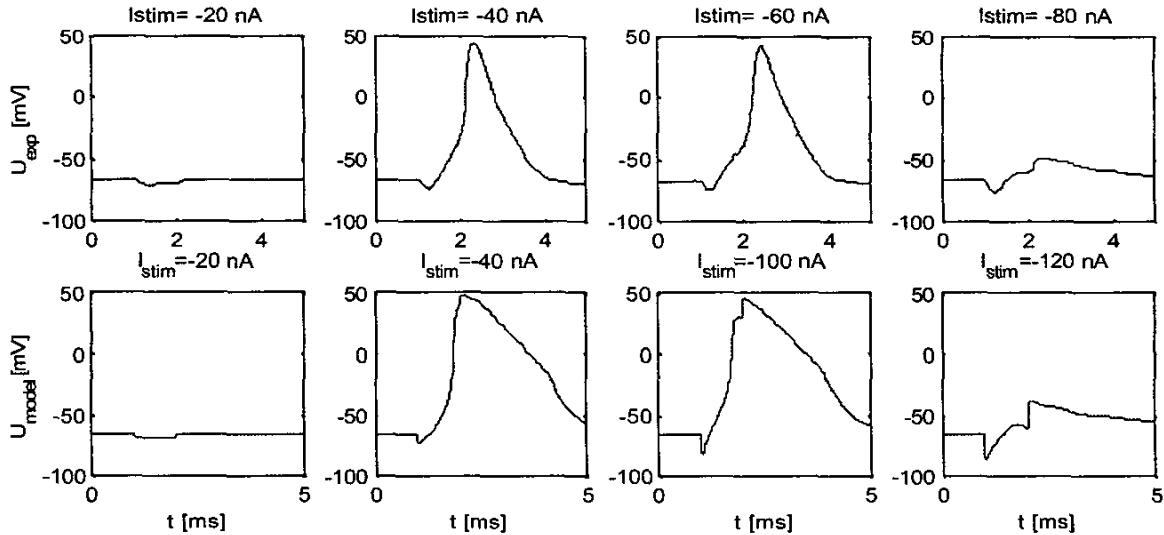


Fig. 4. Upper traces: Extracellular stimulation of a DRG neuron covering an electrode, which is used as a current sink with 1 ms pulses between  $-20$  and  $-80$  nA. After an initial hyperpolarization, the recorded intracellular potential depolarizes and an action potential is generated if the stimulus amplitude is within a window of  $-40$  to  $-60$  nA. Lower traces: The intracellular potential due to extracellular stimulation as simulated with the finite element model.

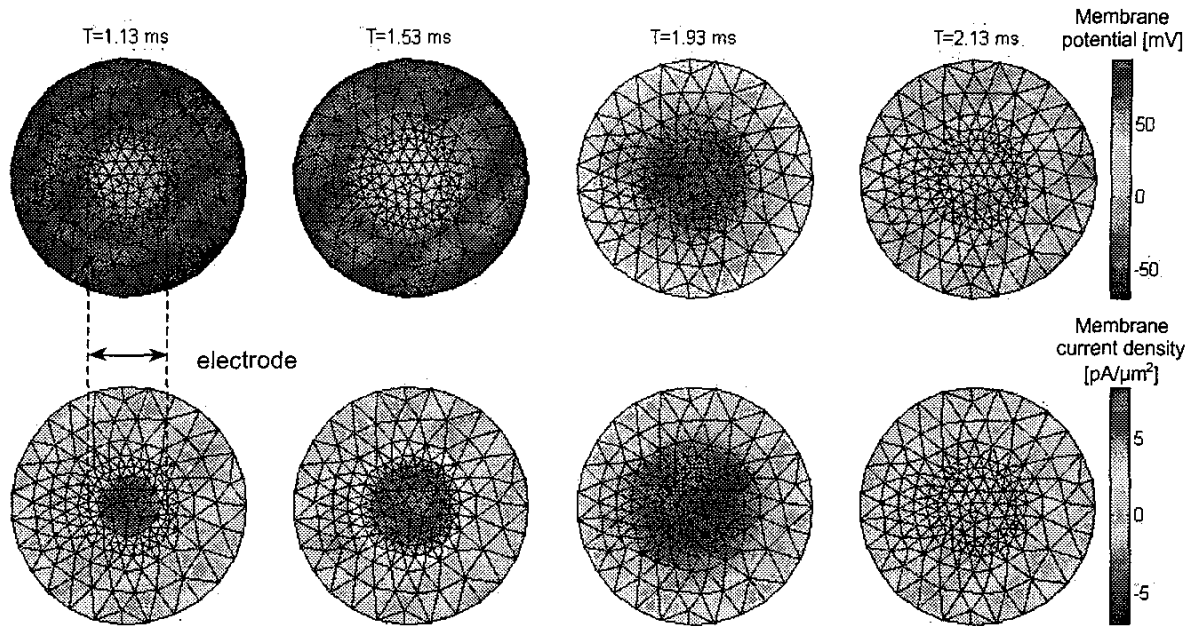


Fig. 5. Simulated distribution of the membrane potential (upper row) and current density (lower row) in the lower membrane at several time instants during stimulation with  $-40$  nA (see fig. 3).

and therefore computed directly from  $u_m$ . The membrane capacity  $C_m$  and ion specific conductances are computed using the membrane area that is represented by each node. Similarly, the time derivatives of the local potentials at the electrode surface are computed assuming capacitive nature of the electrode

$$\frac{du_s}{dt} = \frac{1}{C_e} i_s \quad (6)$$

with  $C_m$ , the electrode capacity for the electrode area represented by each node.

### III. RESULTS

The cultured neuron is stimulated extracellularly by using the electrode as a current sink. For a stimulus amplitude of  $-20$  nA, this results in a hyperpolarisation of the intracellular potential (fig. 4, upper traces). When the stimulus amplitude is increased to  $-40$  nA, the response of the intracellular potential starts with a short period of hyperpolarisation followed by an action potential. The same response is measured with  $-60$  nA stimulation. However, no action potential results from a stimulus of  $-80$  nA.

The stimulation window, as observed in the experimental results is also produced by the finite element model (fig. 4, lower traces). Although the limits are not entirely the same and the dynamic behaviour of the measured intracellular action potential is not fully reproduced, the model will be

used to gain some insight in the biophysical mechanisms involved in the transfer of stimuli to the neuron.

Due to the applied stimulation currents through the sealing gap, the potential in the sealing gap becomes negative with respect to the potential in the rest of the culture medium. As a consequence, the lower membrane potential is depolarized, while the upper membrane (determining the intracellular potential) is slightly hyperpolarized. In the simulations, a stimulus current of  $-40$  nA results in a suprathreshold depolarisation of the lower membrane above the electrode (fig. 5). The opening of voltage dependent sodium channels in this part of the membrane results in a local inward membrane current density. This current, in turn, will depolarize the upper membrane resulting in the generation of an action potential.

In a simulation with a stimulation amplitude of  $-120$  nA, the lower membrane above the electrode is depolarized to a value of  $70$  mV (fig. 6). Since this value exceeds the equilibrium potential for sodium ( $V_{Na}=50$  mV), opening of the voltage sensitive sodium channels will result in an outward instead of an inward current density! In the sealing gap around the electrode, the lower membrane potential radially decreases towards the potential of the upper membrane. An inward current density arises in a ring shaped region around the electrode where the membrane potential is below the sodium equilibrium potential but still above the threshold for opening of channels. Since the total inward membrane current is impaired by the outward current in the part of the membrane above the electrode, the upper

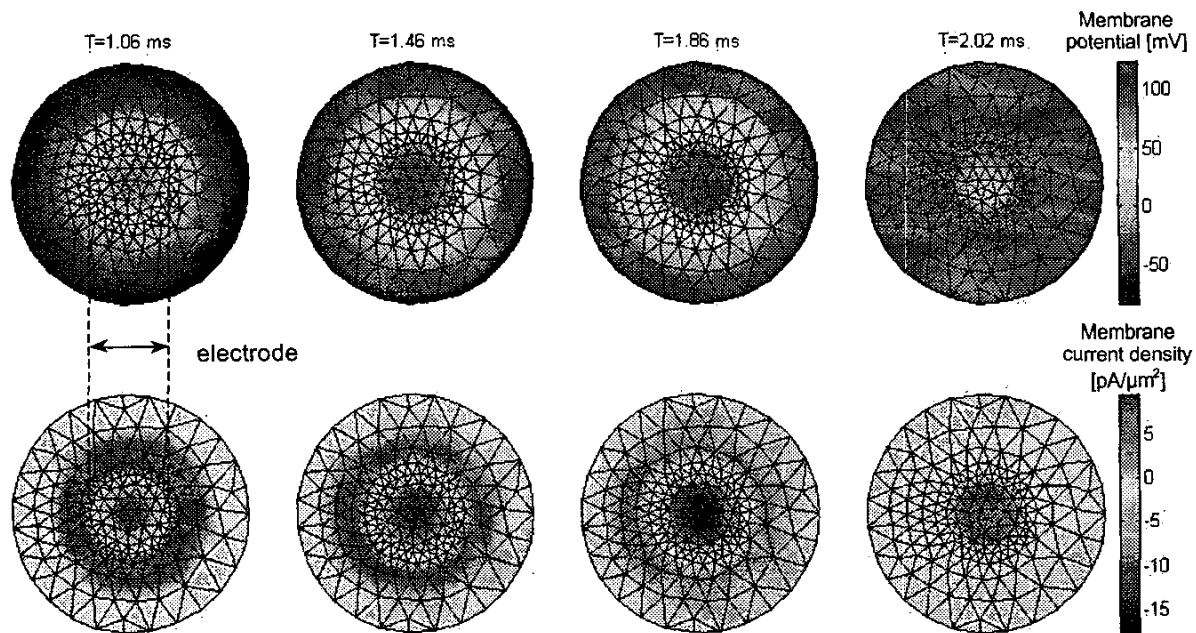


Fig. 5. Simulated distribution of the membrane potential (upper row) and inward current density (lower row) in the lower membrane at several time instants during stimulation with  $-120$  nA (see fig. 3).

membrane can no longer be depolarized far enough for initiation of an action potential.

#### IV. DISCUSSION

The experimental results demonstrate the possibility of extracellular stimulation of action potentials with amplitudes in the nano-ampère range. Some differences exist between the experimental and simulated intracellular potential, due to the assumed geometry and membrane dynamical properties, which are not conform the experimental situation (fig. 4). Nevertheless, the measured initial hyperpolarisation preceding the action potentials can be explained from the simulations. According to the model, this hyperpolarisation is accompanied by depolarisation of the lower membrane, which can not be observed from the intracellular potential. For initiation of an action potential, the lower membrane inward current density, induced by stimulation, should be sufficient for suprathreshold depolarisation of the upper membrane. This sets the lower limit of the stimulation window.

The upper limit of the stimulation window is determined by a complex balance between the inward and outward current densities induced in the lower membrane. Both the amplitudes and the regions over which these current densities are induced depend on the stimulus amplitude.

Ofcourse, both the upper and the lower limit of the stimulation window are also determined by the geometry of the neuron-electrode interface and the electrical properties of the sealing gap and the neuronal membrane. Since finite

element model, used in this paper, is able to compute the dynamic local membrane potentials and current densities for a variety of interface geometries it is a valuable tool for further exploration of the stimulation window.

#### ACKNOWLEDGMENT

The authors wish to thank Kathrin Peters and Marga Deenen for their excellent support of the culturing activities in our lab and Martijn Goedbloed for the fabrication of the MEAs used in the experiments.

#### REFERENCES

- [1] Y. Jimbo, A. Kawana, "Electrical stimulation and recording from cultured neurons using a planar electrode array", *Bioelectrochem. Bioenerg.*, vol. 29, pp. 193-204, 1992.
- [2] J. van Pelt, P. Wolters, D. van Veen, J. Bomer, W.L.C. Rutten, H. Overdijk, G.J.A. Ramakers, "Long-term multielectrode registration of neuronal firing activity from rat cerebral cortex tissue in vitro", *Proc. Int. Conf. IEEE Eng. Med. & Biol. Soc., ISBN 90-9010005-9 (CDROM)*, 1996.
- [3] M. Bove, M. Grattarola, S. Martinoia, G. Verreschi, "Interfacing cultured neurons to planar substrate microelectrodes: characterisation of the neuron-to-microelectrode junction", *Bioel. chem. and Bioen.*, **38**, pp. 255-265, 1995.